K. E. Drangeid

R. Sommerhalder

H. Müller

H. Seitz

Attenuation of a Magnetic Field by a Superconductor

Abstract: Observation of magnetic ac field penetration through superconducting tin films has led to the discovery of a 180° phase shift between the magnetic fields on either side of the film under favorable conditions. This result has so far been published only in a short note, and the present paper presents a detailed description of the experimental technique. A more quantitative discussion, with emphasis on the physical aspects of field attenuation in superconductors, will be published in a future paper.

Introduction

Observation of the penetration of an ac magnetic field through superconducting tin films has led to the discovery of a 180° phase shift between the magnetic fields on either side of the film under favorable conditions. This result, originally predicted by Pippard², gives a straightforward demonstration of a nonlocal Meissner effect in superconductors. These findings have been published only in a short note, and a detailed description of the experimental technique is presented here.

The existence of a nonlocal Meissner effect was derived by Tinkham and Ferrell³ by a method which avoids problems of microscopic theories. The evidence available from direct experimental observation was not extensive, although it was quite suggestive. In view of the fundamental importance of the equation relating the density of the supercurrents to their magnetic vector potential, we believed that additional information would be of interest.

Previous to our experiment, Lewis, Cochran, Frauenfelder, Mapother and Peacock⁴ reported on an unsuccessful attempt to observe, in a superconducting halfspace, magnetic fields which are reversed compared to the externally applied field. Their design was based on the idea that the magnetic field inside the superconductor is detected by angular correlation measurements taken on a monoatomic layer of a suitably chosen radioactive tracer embedded some distance below the surface. The

difficulties of the sample preparation, however, could not be overcome.

Sommerhalder suggested that such negative fields in a superconductor might be detected by measuring the magnetic field which has penetrated a superconducting layer of finite thickness, ⁵⁻⁷ thereby considerably reducing the problems encountered in sample preparation. However, even this simplified arrangement presented difficulties, because in this case the magnetic fields to be detected are smaller by several orders of magnitude (Sommerhalder and Thomas^{8a,8b}), than with the arrangement of Lewis et al. For this reason, sensitive measuring equipment and perfectly compact specimens are needed in order to avoid disturbing magnetic leakage fields.

We briefly recall the outlines of the experimental arrangement (Fig. 1). Tin films were evaporated onto the outside surface of a rotating substrate to obtain long, hollow, cylindrical films. They were then cut from the vacuum system and cooled to liquid helium temperatures. A magnetic ac field H_a at frequency $\nu=1.1\times10^5$ cycles/sec was applied parallel to the axis of the cylinder. The magnetic field H_i which penetrated through the films into the interior of the hollow cyclinder was detected by a pickup coil placed inside the superconducting cylinder. The induced pickup voltage was tuned with an external capacity, amplified in a tuned amplifier and then displayed on a dual beam cathode-ray oscilloscope with ex-

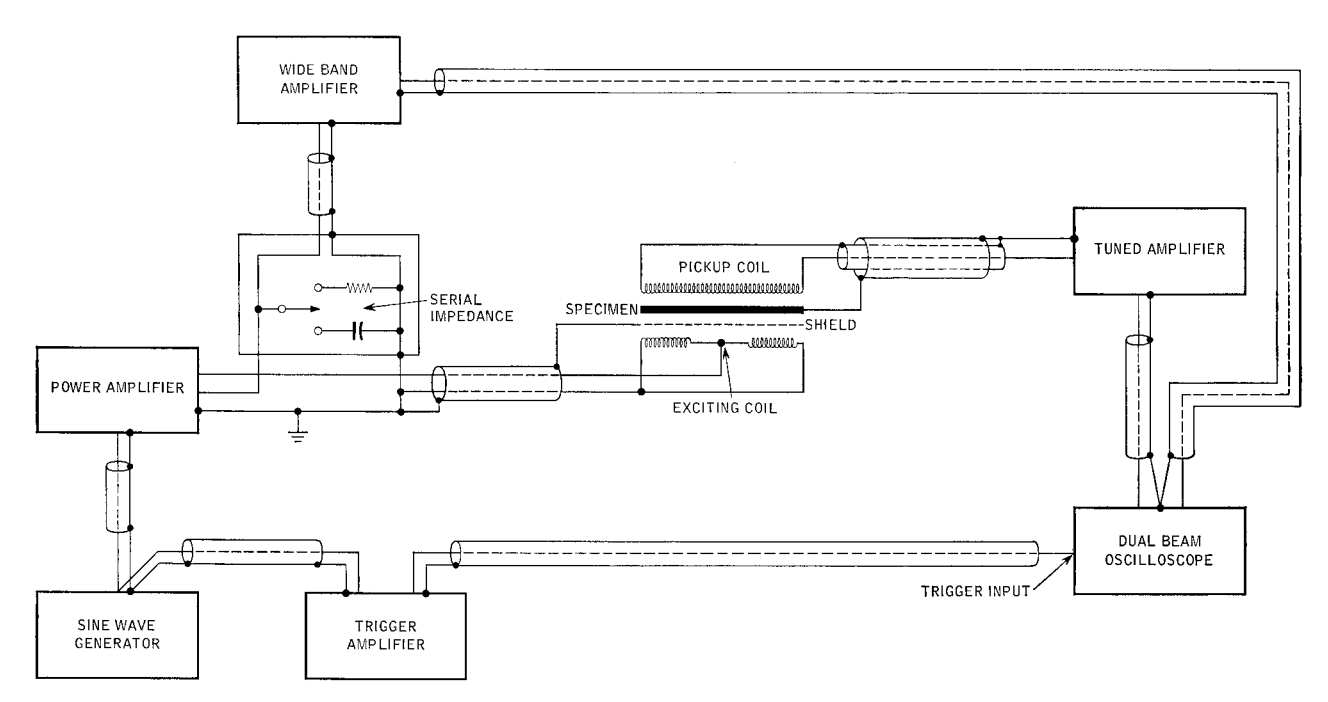


Figure 1 Block diagram of measuring equipment.

ternal triggering, together with a signal indicating the drive current in the exciting field coil. Both the amplitudes and the phases of the two voltages could then be compared simultaneously.

Theory of field attenuation

The field attenuation ratio H_i/H_a was calculated in previous papers, 8a,8b,9 for infinitely long, hollow cylinders of radius R with various parameters such as film thickness, D, penetration depth, λ , and coherence length, ξ . The methods used apply to an arbitrary kernel K relating the density of the supercurrents to their magnetic potential at zero temperature for diffuse or specular surface scattering. Numerical details, however, were worked out only for the case of Pippard's kernel, since the purpose of those calculations was to find the right orders of magnitude for the parameters involved in the construction of the equipment. It seems to us unlikely that significant changes occur if the BCS kernel is introduced rather than the Pippard kernel. 10

We wish to stress here one important point only: In our previous calculations, the interior of the hollow cylinder was assumed to be empty, whereas under experimental conditions it was filled with a tuned pickup coil. But since the impedance in the interior of the hollow cylinder influences the field attenuation ratio, it must be analyzed to permit transformation of the field attenuation ratios we had measured previously to the idealized situation assumed to be valid in our calculations.

In order to work out this procedure, we treat the film as an infinite plane layer perpendicular to an x axis and extending from x = 0 (inside boundary of the hollow cylinder) to x = D (outside boundary). We then find the magnetic field within the film, H(x), from the solution of the equation

$$\frac{d^2A}{dx^2} = \int K(x - x') A(x') dx' \tag{1}$$

for the magnetic vector potential, A(x), by taking its curl $\mu_0 H(x) = dA/dx$.

The limits of integration depend on the special assumptions made for the surface scattering: For diffuse scattering A(x) = 0 in the interval x < 0, x > D; for specular scattering A(x) has to be prolongated symmetrically in this interval.

Boundary conditions for Eq. (1) are

$$A'(0) = \mu_0 H(0) = \mu_0 H_i$$

$$A'(D) = \mu_0 H(D) = \mu_0 H_a$$

A further condition follows from the general relationship between electric field and magnetic vector potential $\mathbf{E} = j\omega \mathbf{A}$. If at x = 0 the electric field is related to the magnetic field by means of

$$z_L = E(0)/H(0),$$
 (2)

the impedance of the interior of the cylinder, we then find $A(0) = H_i z_L/j\omega\mu_0$.

14

The field attenuation ratio turns out to be^{8a, b}

$$\frac{H_i}{H_a} = \frac{\psi(0)}{2\psi(D)} \times \frac{2j\omega\mu_0\xi\psi(D)}{z_L + j\omega\mu_0\xi\psi(D)}$$
(3)

for both types of surface scattering, where ψ is a solution of Eq. (1) with boundary conditions $\psi'(0) = 0$ and $\psi'(D) = 1$.

Equation (3) specializes to

$$\frac{H_i}{H_a} = \frac{1}{2 \cosh (D/\lambda)} \frac{2j\omega\mu_0\lambda \coth (D/\lambda)}{z_L + j\omega\mu_0\lambda \coth (D/\lambda)}$$
(4)

in the London limit $\xi \rightarrow 0$, and further to

$$\frac{H_i}{H_a} = e^{-D/\lambda} \frac{2j\omega\mu_0\lambda}{z_L + j\omega\mu_0\lambda} \tag{5}$$

for $D \gg \lambda$. If instead of a superconductor a normal conductor with resistivity ρ^* is considered, λ has to be replaced by

$$\alpha = \sqrt{\rho^*/2\mu_0\omega} (1-j) \tag{6}$$

provided that the wall thickness D of the specimen and the skin effect penetration depth $\delta = \sqrt{2\rho^*/\mu_0\omega}$ are much smaller than the radius R of the specimen.

Equation (5) suggests a rather intuitive interpretation. The first factor represents the field attenuation ratio of an electromagnetic plane wave which has penetrated the film from its outside to its inside, whereas the second factor represents the transmission factor of this wave as it penetrates from the inside boundary of the film with impedance $z_0 = j\omega\mu_0\lambda$ or $z_0 = j\omega\mu_0\alpha$, respectively, into the hole with impedance z_L . A formally similar interpretation holds when Eq. (3) is considered instead of Eq. (5). The impedance z_L must be determined from the data of the equipment. In the case of an empty hole $z_L = j\omega\mu_0 R/2$.

Electrical equipment

• Experimental arrangement

Details of the coil system and of the film mounting are shown in Fig. 2. The current for the exciting field H_a was produced by a sine wave generator; a maximum field strength of $H_a=30$ Oe was available. The drive coil (length 90 mm, diameter 34 mm) was made of copper wire wound on a glass core. It consisted of two halves, with 130 turns each, connected in parallel (Fig. 1) in order to keep both ends of the coil at ground potential. It was found that a layer of baked-in conductive silver on the core was necessary to eliminate capacitive disturbances. Only a negligible attenuation of H_a through this layer was observed even at liquid helium temperatures.

The pickup coil was wound on plexiglas; the inner core

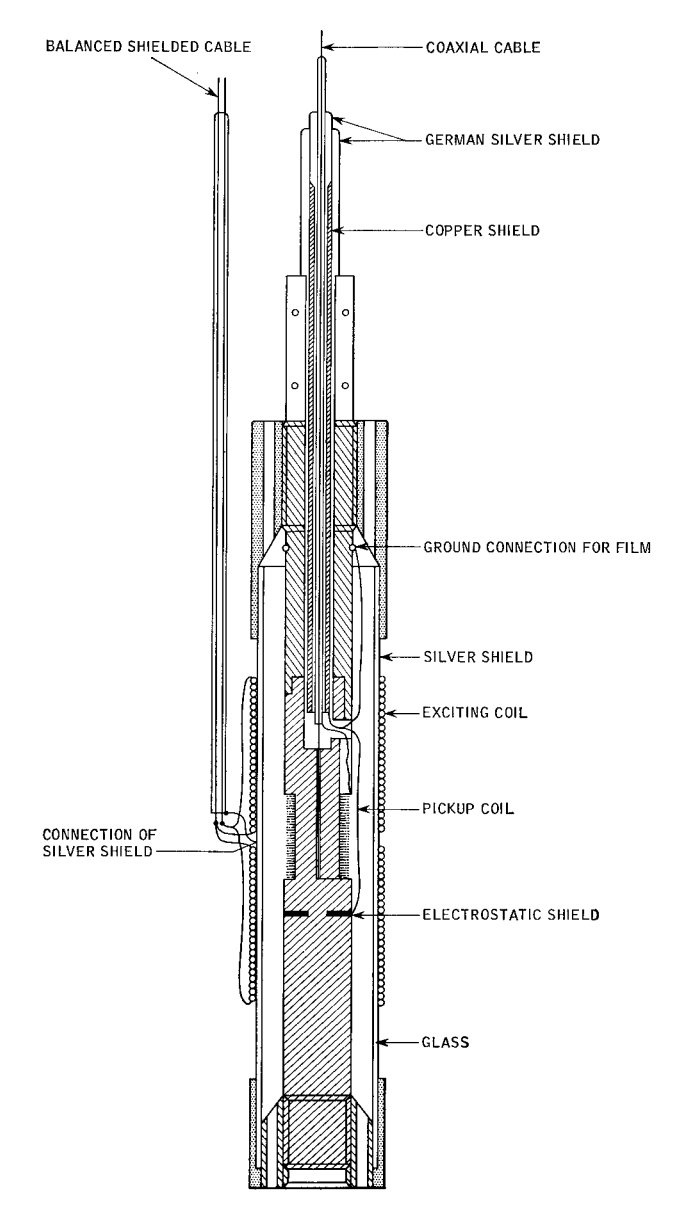


Figure 2 Coil system and film mounting.

diameter was 12 mm, the outer, 18 mm, and the length of the coil 24 mm. There were 898 turns of copper wire consisting of 20 isolated filaments, each 0.04 mm in diameter. Current connection to the pickup coil was made through a shielded coaxial cable. Moreover, this cable was shielded by a copper tube about 1 mm thick. A capacitive shield was placed below the pickup coil.

Our film substrates were polished pyrex tubes (length 150 mm, outer diameter ≈ 22 mm). They were fitted into the coil system as indicated in Fig. 2 and grounded by a wire soldered to a baked-in conductive silver spot on the substrate. Special attention was given to the ground connections of the system, as shown in detail in Fig. 1.

• Determination of the hole impedance

A series of experiments was performed to determine the hole impedance, z_L . For this purpose, the current leads to the exciting coil were disconnected and current was fed into the pickup coil. Then the pickup coil may be considered as the transformer primary and the specimen as the secondary. The equivalent circuit diagram is shown in Fig. 3. Here, ρ is the dc resistance of the pickup coil, r and L are the resistance and inductance of the specimen, respectively. L_1 , L_2 and L_3 are the inductances corresponding to the fluxes ϕ_1 , ϕ_2 and ϕ_3 as indicated in Fig. 4.

Since u, the voltage ratio of the primary with the secondary side of the transformer, is arbitrary, we may put L_1 equal to L_3 without loss of generality. Let us denote by z_L ' the ratio of voltage to current between A and B in Fig. 3. The ratio z_L ' is proportional to the hole impedance z_L defined by Eq. (2), the constant of proportionality being defined by the geometry of specimen and coil system. If the length l of the pickup coil were much larger than the inner radius R of the specimen, then clearly

$$z_L = \frac{2\pi R}{I} z_L. \tag{7}$$

We believe this relation did hold quite accurately in our arrangement, because the diameter of the pickup coil was close to the radius of the specimen. This idea was also confirmed by the fact that no change of z_L ' was observed when the specimen was lowered until its upper end was on the same level as the upper end of the pickup coil.

In order to determine L_1 and L_2 , the pickup coil was tuned with a Q-meter at various frequencies and for two different types of load impedance: (a) no load, and (b) a superconducting tin film. In each case the reciprocal square of the resonant frequency was plotted versus the additional capacitance needed to produce resonance; one finds then a straight line with a slope φ , where

$$\tan \varphi_a = L_1 + L_1 L_2 / (L_1 + L_2)$$
 and $\tan \varphi_b = L_1 + L_2$, (8)

respectively. Note that $(L_1 + L_2)$ is the self-inductance of the secondary side seen from its primary side.

Now if $(L_1 + L_2)'$ is the self-inductance of the secondary, and if we remember $L_1 = L_3$, we obtain u from the ratio

$$(L_1 + L_2)/(L_1' + L_2') = u^2. (9)$$

For very large ratios l/R clearly

$$(L_1 + L_2)' = \mu_0 \pi R^2 / l. \tag{10}$$

In our arrangement, however, $l/R \approx 1$. A corrected

value of the self-inductance $(L_1 + L_2)'$ was, therefore, taken from the tables of Terman.¹²

Now the components of the transformer circuit are determined. A check of its validity was made by introducing as a third type of load impedance a thick-walled normal conducting specimen of a known dc resistivity ρ^* . A short calculation leads in this case to the expression

$$z_{L'} = [K \cdot L_2^2 / (L_1 + L_2)^2] \cdot \sqrt{\nu}$$
 (11)

for the hole impedance z_L' at resonance frequency, where $K=2\pi R/l\cdot\sqrt{\pi\mu_0\rho^*}$ contains only the coil geometry data and the dc resistivity of the specimen¹³. If the expression for $L_2^2/(L_1+L_2)=\tan\varphi_b-\tan\varphi_a$ is taken from Eq. (8), we arrive at

$$z_{L'} = [K/(L_1 + L_2)] \cdot (\tan \varphi_b - \tan \varphi_a) \cdot \sqrt{\nu},$$
 (12)

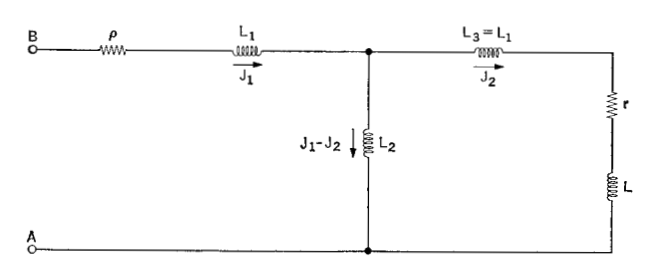
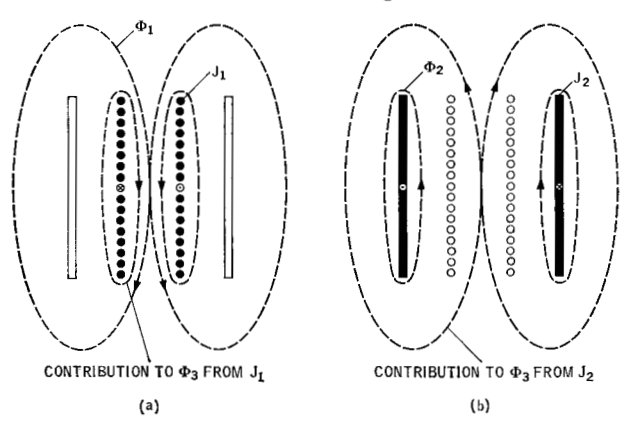
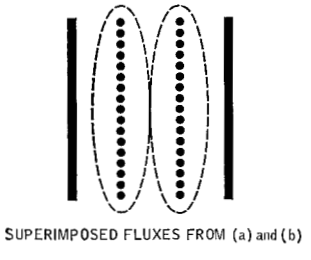


Figure 3 Equivalent circuit diagram of driven pickup coil in a specimen.

Figure 4 Transformer flux diagram.





(c)

so that from a plot of z_L' at resonance versus the square root of the resonant frequency, we may determine $K/(L_1 + L_2)$, which is invariant against a change of u.

Figure 5 gives the results for a pickup coil in a brass specimen at room temperature. We find $K/(L_1 + L_2) = 108.5$, which compares well with the calculated value 108.1. The accuracy of our Q-meter in a single measurement was about 10%.

• Field attenuation measurement

Let us now return to the original arrangement of Fig. 1, where current is fed into the exciting coil and where the voltage induced in the pickup coil is tuned to maximum with an external capacitance C.

Starting with the field attenuation formula for a normal conductor developed in the section "Theory of Field Attenuation," we have

$$H_i/H_a = e^{-D/\alpha}[2z_0/(z_0 + z_L)],$$
 (13)

where

$$z_0 = j\mu_0\omega\alpha, \tag{14}$$

we find with reference to Eq. (2) the electric field E_i at the inside boundary of the specimen to be

$$E_i = H_a e^{-D/\alpha} z_L [2z_0/(z_0 + z_L)].$$

If now z_L is substituted by $z_{L'}$ in Eq. (7), if a similar transformation

$$z_0' = z_0 2\pi R/l \tag{15}$$

is carried out with z_0 , and if E_i is replaced by the voltage $U_i = 2\pi R E_i$ at the inside boundary of the specimen, then

$$U_{i} = 2H_{e}e^{-D/\alpha}z_{0}'l[z_{L}'/(z_{L}'+z_{0}')].$$

Thus the equivalent circuit diagram of Fig. 6 may be introduced. Here, U stands for

$$U = 2z_0' H_a l e^{-D/\alpha}. {16}$$

Note that U is an impressed voltage which remains constant if the voltage U_c of the capacitance C is set to maximum. Having performed some simple calculations we arrive at a maximum voltage

$$U_{c} = -Uj\omega L_{2} \frac{[\omega^{2}L_{1}(L_{1}+2L_{2})-r\rho]}{[\omega^{2}L_{2}^{2}r+\omega^{2}(L_{1}+L_{2})^{2}\rho+r^{2}\rho]} \cdot (17)$$

This formula was again carefully checked with normal conducting specimens such as copper, aluminum and brass at various temperatures from room temperature down to liquid helium temperatures.

We illustrate the results found with brass at room temperature. For a set of specimens all cut from the same rod and having the same inner radius R, U was measured with respect to phase and amplitude as a function of the different wall thicknesses D of the set. From these plots

Table 1 α values of brass at room temperature.

Method	α
Field attenuation ratio measurement	$\alpha_{\rm real\ part} = 0.39\ {\rm mm}$
Phase shift measurement	$\alpha_{\rm imaginarypart} = 0.38{\rm mm}$
Theoretical value computed from measured dc resistivity, $\rho^* = 6.43 \cdot 10^{-8} \Omega \text{m}$	$\alpha_{\text{real part}} = $ $\alpha_{\text{imaginary part}} = 0.38_5 \text{mm}$

 α was evaluated (see Table 1) according to Eq. (16), and z_0' was computed with Eqs. (14) and (15). Finally, the voltage U_c of the capacity was calculated from Eq. (17).

Our arrangement was designed as listed below:

$$R = 0.97_5 \text{ cm}$$
 $L_2 = 1.33 \times 10^{-3} \text{ Hy}$
 $l = 2.4 \text{ cm}$ $\rho = 19\Omega$
 $\omega = 2\pi \times 1.1 \times 10^5 \text{ c.p.s.}$ $r = 77\Omega$
 $L_1 = 0.67_5 \times 10^{-3} \text{ Hy}$ $H_a = 8.67 \text{ A/cm}$

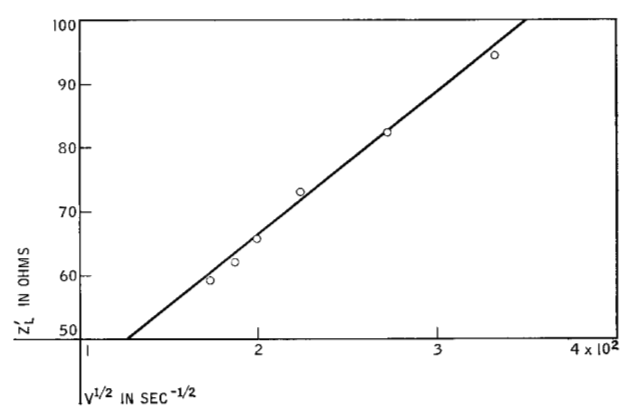
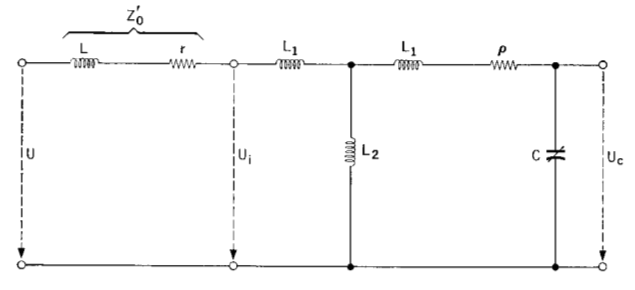


Figure 5 Hole impedance $\mathbf{z_L}'$ at resonance as a function of frequency, for brass at room temperature.

Figure 6 Equivalent circuit diagram of tuned pickup coil in a specimen.



With these data we calculated $U_c = 0.69$ V for D = 2 mm, which increases to $U_c = 0.73$ V if the Bessel function correction is applied. This is to be compared with the measured voltage $U_c = 0.76$ V, we conclude from this result that we can be confident about our analysis. Equation (17) simplifies to

$$U_c = -j\omega U L_2 (L_1 + 2L_2) L_1 / (L_1 + L_2)^2 \rho$$
 (18)

for a superconductor.

We now relate U to the ideal field attenuation ratio that would be present if no pickup coil system were used. Then clearly

$$U = -[(H_i/H_a)_{ideal}][H_a\mu_0\pi R^2\omega j]. \tag{19}$$

If we substitute Eq. (19) into Eq. (18) and simultaneously introduce a voltage ratio u between primary and secondary coil and an amplification factor v for the tuned amplifier, we finally get

$$(H_i/H_o)_{ideal} = U_c \frac{1}{j\mu_0\pi R^2 H_a \omega} \frac{1}{v} \frac{\rho}{\omega L_1 u} \frac{(L_1 + L_2)^2}{(L_1 + 2L_2)^2}.$$
(20)

This result may be interpreted essentially as the ratio of the voltages induced at the ends of the pickup coil (with and without a specimen, respectively) divided by the product of the *Q*-factor of the pickup coil with the amplification factor of the tuned amplifier.

Note that our previously published field attenuation ratios were not yet based on Eq. (20), but on a less refined analysis. According to Eq. (19) the sensitivity of our equipment (see Fig. 1 of Ref. 1) was $H_a/H_i = 3.8 \times 10^9$ instead of 1.0×10^9 . Data for u and v in our arrangement were u = 427 and $v = 2 \times 10^6$.

Sample preparation

Our specimens were tin films evaporated onto the outside of polished pyrex tubes (length 15 cm, outside diameter ≈22 mm). From the result of our numerical calculations we concluded that a coherence length ξ as large as possible is highly desirable. One is tempted, therefore, to expect good specimens if the films are evaporated at a low evaporation rate in an ultrahigh vacuum and subsequently annealed, in order to produce large crystallites with a small amount of disorder. Films prepared in this manner have a residual resistance of the order of some thousandths of the room temperature resistance (see also Ref. 14), but the low density of nucleation sites makes it difficult to form continuous films less than about 1000 A on room temperature substrates. Moreover, films annealed above room temperature show a tendency to break up, at least partly. We found that films prepared under conditions as mentioned above showed appreciable leakage in magnetic shielding power and, therefore, had to be discarded.

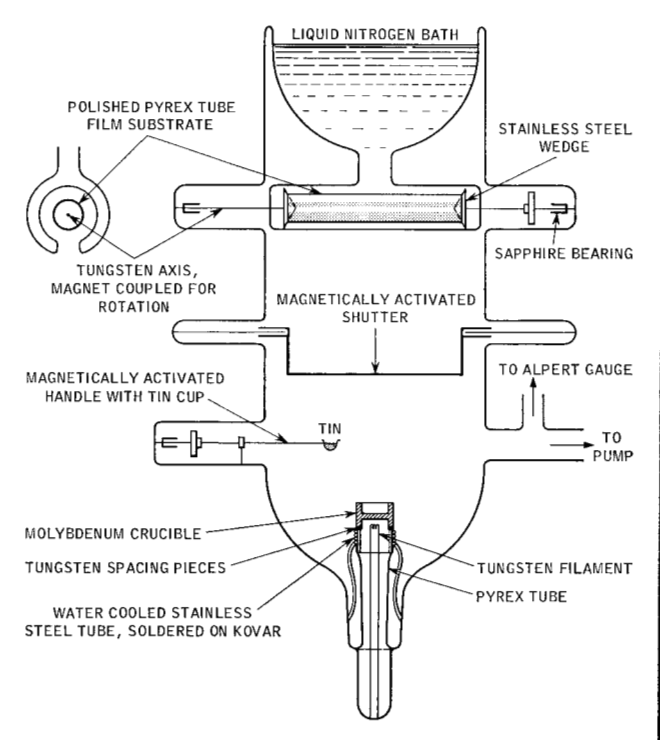


Figure 7 Vacuum equipment.

In order to obtain smoother, continuous films, we introduced an extremely high evaporation rate, rather than a low one, and the substrates were prevented from heating above room temperature during evaporation by a liquid-nitrogen-cooled screen around the substrate. Furthermore, we introduced additional nucleation sites by coating the substrates with a thin layer of tin oxide. This preparation technique is partly contradictory to that required for specimens with a large coherence length, but we found that the technological compromise had to greatly favor smooth films rather than films with a large mean free path. The resistivity behavior of some samples is listed in Table 2.

Details of the vacuum system are shown in Fig. 7. An

Table 2 Temperature dependence of film resistance.

Film thickness	Residual resistance ratio	
	$R(77^{\circ}K)/R(300^{\circ}K)$	$R(4^{\circ}K)/R(300^{\circ}K)$
3,900 A	0.17	0.022
6,400	0.19	0.022
10,400	0.15	0.0084
10,500	0.23	0.023
18,700	0.24	0.032
35,000	0.175	0.028

all-glass ultrahigh vacuum equipment was used with an oil diffusion pump and a liquid nitrogen cooling trap. A pressure of the order of 10^{-9} mm Hg was measured on the Alpert gauge.

The crucible, a molybdenum cup placed loosely on a water-cooled Kovar ring, was heated by electron bombardment. A stabilized power supply of 1.5 kw was available, permitting flashing temperatures up to the melting point of molybdenum. A pyrex tube below the cooled Kovar ring prevented the electrons from ionizing tin during the evaporation.

The pyrex substrate tubes were mounted on a tungsten axis with two wedges of stainless steel and were held in sapphire bearings. The axis was rotated by magnets driven with a motor mounted outside.

Careful attention was given to the outgassing procedure. After the usual outbaking of the whole system at 400 to 450 °C for several hours, the empty crucible was flashed to high temperatures until a pressure rise was no longer observed.

Although our evaporation source consisted of a very hot metal in contact with a cooled one, it worked very satisfactorily if thermal contact was reduced by inserting small spacing pieces of tungsten between Kovar and molybdenum.

The tin was kept in a movable glass cup. It was melted by radiation heat from the crucible and transferred into the outgassed molybdenum crucible. Approximately one-third was evaporated on the closed shutter. Then the cooling trap on top of the system was filled with liquid nitrogen and left for three to four hours. A temperature of $\approx -100\,^{\circ}\mathrm{C}$ at the substrate could be realized in this manner. Then the crucible was again powered, the tin evaporated during the warming up period having condensed on the closed shutter.

When the shutter was opened, the electron bombardment power and the pressure indicated by the Alpert gauge were recorded simultaneously. Film thicknesses obtained could be estimated roughly from the recorded product of bombardment power with evaporation time.

Films about 10,000 A thick could be produced in about 10 sec. Considering the distance d=20 cm between crucible and substrate, and the fact that most of the (rotating) total substrate surface was not exposed to the condensing tin vapor, this corresponds to a high evaporation rate at the crucible. Note that no appreciable pressure rise was recorded during evaporation (see Fig. 8), which is contrary to the often mentioned inherent difficulty of outgassing tin. $^{14.15}$

It should be noted that after evaporation there was always a noticeable amount of tin oxide in the otherwise empty crucible, but we suspect that our tin films were far from being oxide-free.

Film thicknesses were determined from the measure-

ment of the electric losses in a *Q*-meter at room temperature, the analysis being much the same as was worked out previously in the section "Electrical Equipment." Test measurement results obtained from chemical analysis indicated that the resistivity of the films corresponds within 20% to the bulk value, a large contribution to this error being caused by uncertainties arising from the chemical analysis.

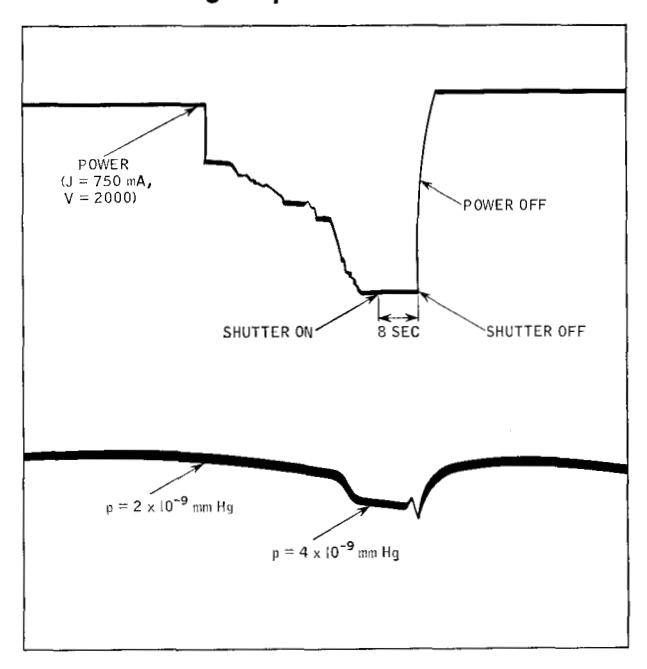
The distribution of holes in our films was examined in a dark room with a source of illumination in the interior of the hollow cylinder.

Films with isolated spots from distilled water, tin oxide, dust, grease, scratches or local faults in the glass were discarded. Among the remaining specimens a large scattering in the content of small holes was found, which we could not relate to definitely different conditions during evaporation. But since the hole content is very important for the measurement, we are left with the fact that the conditions necessary for preparation of good specimens were poorly understood.

Discussion of results

Pippard² pointed out as early as 1953 that a nonlocal electrodynamics of the superconducting state leads to a Meissner effect in which the externally applied magnetic field is not only attenuated in the superconductor, but undergoes a region of (small) negative fields until it reaches its asymptotic zero value, provided the coherence

Figure 8 Copy drawing of recorder plot of bombardment power and vacuum pressure during evaporation.



length, ξ , is larger than the penetration depth, λ . He also stressed that the existence of this negative magnetic field region depends on the general hypothesis that the density of the supercurrents is determined by some sort of space average of the magnetic vector potential, but not on the special form of the integral kernel introducing this average. The importance of a straightforward experimental proof of a nonlocal electrodynamics in the superconducting state motivated this work. We give here an intuitive picture of Pippard's statements, referring for a more critical description to the calculations made in a previous section

Suppose a superconducting half-space with its surface in the (y, z)-plane and the x-axis pointing towards the interior of the specimen. According to London's local theory ($\xi = 0$), there would be an exponential attenuation of an externally applied magnetic field, $H_c(x) = H$, and also of the magnetic vector potential, $A_v(x) = A$, with increasing distance, x, from the surface (Fig. 9).

At any position x_0 , the supercurrents, $j_{\nu}(x) = j$, may be derived from either H or A. If for simplicity we assume the factors of proportionality to be unity, we find

$$j(x_0) = dH(x_0)/dx (21)$$

and

$$j(x_0) = A(x_0) \tag{22}$$

from Maxwell's and London's equations, respectively, (div A=0).

We will now modify this picture into that of the non-local theory by increasing smoothly the coherence length. While Eq. (21) clearly holds also under nonlocal conditions, Eq. (22) then changes to

$$j(x_0) = \bar{A}^{\xi}, \tag{23}$$

the superscript denoting a mean value taken around x_0 within a distance ξ , the coherence length.¹⁶

Now, as long as A(x) is a convex function, $(d^2A/dx^2 > 0)$, it has the property $|\bar{A}^{\xi}| > |A(x_0)|$ (see Fig. 9). This means that the current density in the nonlocal case is larger than in the local one, which implies from Eq. (21) that the field attenuation per unit length in the nonlocal case is faster than in the local one. This effect becomes all the more pronounced as the coherence distance becomes larger when compared to the penetration depth, and provided that $x_0 \gg \xi$, so that the mean value formation is not affected by the presence of the surface of the specimen.

Since the asymptotic values of H, A and j are the same in both local and nonlocal situations, one might expect in Fig. 9 a nonlocal modification of the field penetration curve, as is indicated by the dotted lines.

We now give a heuristic argument that this is impossible if the coherence length becomes large compared to the

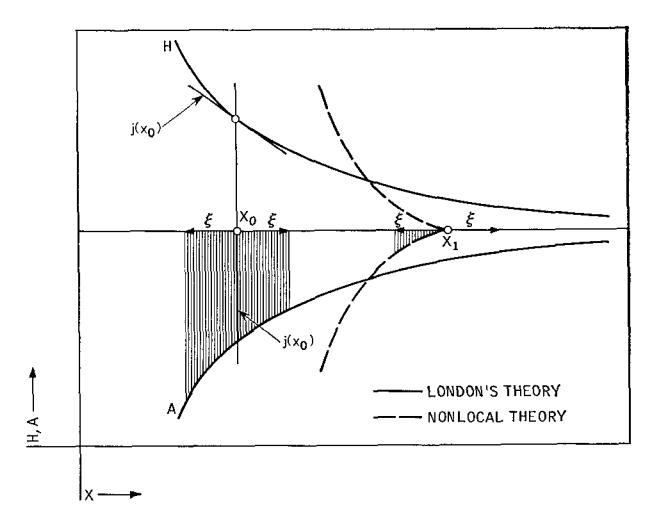


Figure 9 Magnetic field penetration curve in a superconducting half-space: _____ London's theory. __ Nonlocal theory.

depth of field penetration: If x_1 is so chosen in the region $dH/dx \approx 0$ that within a coherence length on its left-hand side we have essentially $A \neq 0$, whereas within a coherence length on its right-hand side we have essentially $A \approx 0$, we would obtain from Eq. (23) a current density $j(x_1) \neq 0$, contrary to $j(x_1) \approx 0$ as derived from Eq. (21). The contradiction is removed, however, as soon as a negative magnetic field at x_1 is introduced.

We see, therefore, that the existence of negative magnetic fields in the superconductor is an immediate consequence of some geometric "inertness" of the supercurrents, which is itself a straightforward consequence of the postulate of a coherence length in the superconducting state.

Since the results we believe to have found are mainly qualitative and were already summarized in an earlier paper, we are not repeating them here. We merely add that the rather thick film ($D \approx 18,700 \text{ A}$), showing negative attenuated fields, implies that $\lambda_P = \xi_0^{1/3} \times \lambda_L^{2/3}$, which is essentially the Pippard penetration depth in an ideal crystal, was nearly equal to the coherence length, ξ , in the film, where ξ_0 is the coherence length in an ideal crystal and λ_L is the London penetration depth. If we assume $\xi_0 = 2500 \text{ A}$ and $\lambda_L = 500 \text{ A}$, we find $\lambda_P = 850 \text{ A}$, which seems to be a reasonable value for the coherence length in the film.

We do not believe that a quantitative discussion of field attenuation measurements, although possible for various film thicknesses and temperatures or in a superimposed dc magnetic field, results in a sound understanding of the relation between the density of the supercurrents and their vector potential, unless these measurements are combined with additional information taken simultaneously on the same specimen, so that two parameters (for

instance, penetration depth, and coherence length) may be determined separately. Our present efforts are directed towards this problem, taking the most elegant method of Schawlow and Devlin¹⁷ as a supplementary technique. However, we should like to postpone the discussion of these results for publication in a future paper.

Finally we recall that the weakest point in our experiments was the technique of sample preparation. We do not know a recipe to eliminate the small holes in the films which may cause a positive magnetic leakage field in the hole of the specimen, covering smaller negative fields that might exist. Our previously published results were taken on the best hole-free specimens we produced, in a set of at least 25 films; the others, however, gave support to our analysis in so far that the phase shift between H_a and H_i was always negligibly small and never showed a noticeable temperature dependence from the critical temperature down to $1.5\,^{\circ}$ K.

References and footnotes

- K E. Drangeid and R. Sommerhalder, Phys. Rev. Letters 8, 467 (1962).
- 2. A. B. Pippard, Proc. Roy. Soc. (London) A216, 547 (1953).
- M. Tinkham and R. A. Ferrell, Phys. Rev. Letters 2, 331 (1959).
- H. R. Lewis, J. F. Cochran, H. Frauenfelder, D. E. Mapother, and R. N. Peacock, Z. Phys. 158, 26 (1960).
- 5. A. L. Schawlow, Phys. Rev. 109, 1856 (1958).

- R. Jaggi and R. Sommerhalder, *Helv. Phys. Acta* 31, 292 (1958).
- E. Erlbach, R. L. Garwin, and M. P. Sarachik, *Bull. Am. Phys. Soc.*, Ser. II, 3, 133 (1958).
- R. Sommerhalder and H. Thomas, Helv. Phys. Acta 34, 29 (1961).
- R. Sommerhalder and H. Thomas, *Helv. Phys. Acta* 34, 265 (1961).
- 9. K. E. Drangeid, M. C. Gutzwiller, R. Sommerhalder, and H. Thomas, "Electric and Magnetic Properties of Thin Metallic Layers," *Koninklijke Vlaamse Academie voor Wetenschappen von Belgie*, Brussels, 1961, p. 326.
- Also discussed by W. Liniger and F. Odeh, unpublished report. (See also *Phys. Rev. Letters* 10, 47 (1963).
- 11. The resistivity of this coil was found to depend upon the magnetic field distribution around the windings. This, however, does not affect any of our conclusions. Furthermore, the skin effect is removed if one filament is used, rather than several parallel filaments.
- F. E. Terman, Radio Engineers Handbook, McGraw-Hill, New York, 1943, p. 54.
- 13. A correction term accounting for the curvature of the assumed plane layer specimen was introduced where necessary but it did not prove to be very important.
- 14. H. L. Caswell, J. Appl. Phys. 32, 105 (1961).
- 15. H. L. Caswell, Rev. Sci. Instr. 30, 1054 (1959).
- 16. Although Eq. (22) is local in j and A, this involves a highly nonlocal relation in the physical quantities j and H. If we accept here Pippard's original intuitive picture, we do not violate our experimental conclusions.
- A. L. Schawlow and G. E. Devlin, *Phys. Rev.* 113, 120 (1959).

Received July 8, 1963